ТЕХНОЛОГИЯ ХИМИЧЕСКОЙ ПЕРЕРАБОТКИ ДРЕВЕСИНЫ И ПРОИЗВОДСТВО ДРЕВЕСНО-ПОЛИМЕРНЫХ КОМПОЗИТОВ

Original article
УДК 662.71
DOI: 10.37482/0536-1036-2026-5-152-166

Characterization of Tar and Biochar as By-Products of Rubberwood (*Hevea brasiliensis*) Pellet Gasification

Wahyu Hidayat*[1]✉*, Doctor of Forest Biomaterials Engineering, Prof.;
ResearcherID: F-8410-2017, ORCID: https://orcid.org/0000-0002-6015-1623
Fadilla Martha Amelia*[1]*, Postgraduate Student; ResearcherID: OSI-7581-2025,
ORCID: https://orcid.org/0009-0005-7500-3825
Hendra Prasetia*[2]*, Doctor of Science and Engineering, Principal Researcher;
ORCID: https://orcid.org/0000-0002-3230-7918
Indra Gumay Febryano*[1]*, Doctor of Forestry, Prof.; ResearcherID: AAW-4454-2021,
ORCID: https://orcid.org/0000-0001-7242-656X
Bugae Park*[3]*, Head of Research and Development Department;
ORCID: https://orcid.org/0000-0002-4626-2351
Agus Haryanto*[1]*, Doctor of Agricultural Engineering, Prof.;
ORCID: https://orcid.org/0000-0002-8954-4463
[1]University of Lampung, Bandar Lampung, Indonesia; wahyu.hidayat@fp.unila.ac.id✉, fadillamarthaa@gmail.com, indra.gumay@fp.unila.ac.id, agus.haryanto@fp.unila.ac.id
[2]National Research and Innovation Agency (BRIN), South Lampung, Indonesia; hend051@brin.go.id
[3]SunBrand Industrial Inc., Jeollanam Province, Republic of Korea; bu2000@hanmail.net

Received on January 9, 2026 / Approved after reviewing on April 3, 2026 / Accepted on April 6, 2026

Abstract. Gasification of rubberwood (*Hevea brasiliensis*) pellets represents a promising pathway for valorizing abundant lignocellulosic biomass into a renewable energy source. In addition to producing synthesis gas (syngas), the process generates by-products such as tar and biochar, which require comprehensive characterization to support process optimization and downstream utilization. The downdraft gasifier was chosen because it produces less tar than other types of gasifiers. This study aims to analyze the chemical composition and characteristics of tar and biochar as by-products of wood pellet gasification of *Hevea brasiliensis* using a downdraft gasifier. Tar chemical components were analyzed using GC-MS, and biochar characteristics were analyzed using XRD, FTIR, and FE-SEM/EDS. The chemical composition of tar comprises complex compounds, including carboxylic acids, alkanes, aromatic hydrocarbons, and phenols. The FTIR spectrum reveals that biochar is characterized by functional groups associated with oxygenated hydrocarbons, which reflect the structural components of carbohydrates, cellulose, and hemicellulose (C−O, C=O, C−H, C=C, C≡C, and C−N). The XRD pattern shows four diffraction peaks, including two sharp and intense peaks ($2\theta = 28°$ and 40°), with the highest crystallinity peak of 71.73 % and a crystal size of 5.47 nm. The biochar structure was analyzed using SEM, revealing scattered pore-like holes and grooves at 1000× magnification, and flakes with pebble-like shapes at 5000×. The chemical elements detected in biochar include carbon,

This is an open access article distributed under the CC BY 4.0 license

oxygen, aluminium, silicon, potassium, calcium, and iron. The major element is carbon, with an atomic percentage of 80.97 %.

Keywords: tar, biochar, downdraft gasifier, rubberwood pellets, GC-MS, XRD, FTIR, FE-SEM/EDS

Acknowledgments: The authors sincerely thank the Korea Institute of Energy Research (KIER) for the generous support through the provision of a 20 kW Gasifier and Syngas Generator, granted under Grant Letter No. KIER-2023-05-03-01. This support greatly contributed to the successful completion of this study.

For citation: Hidayat W., Amelia F.M., Prasetia H., Febryano I.G., Park B., Haryanto A. Characterization of Tar and Biochar as By-Products of Rubberwood (*Hevea brasiliensis*) Pellet Gasification. *Lesnoy Zhurnal* = Russian Forestry Journal, 2026, no. 5, pp. 152–166. (In Russ.). https://doi.org/10.37482/0536-1036-2026-5-152-166

Научная статья

Характеристика дегтя и биоугля при газификации гранул *Hevea brasiliensis*

Вахью Хидаят*[1]✉, *д-р техн. наук, проф.; ResearcherID: F-8410-2017,
ORCID: https://orcid.org/0000-0002-6015-1623
Фадилла Марта Амелия*[1], *аспирант; ResearcherID: OSI-7581-2025,
ORCID: https://orcid.org/0009-0005-7500-3825
Хендра Прасетиа*[2], *д-р естеств. и техн. наук, гл. науч. сотр.;
ORCID: https://orcid.org/0000-0002-3230-7918
Индра Гумай Фебрияно*[1], *д-р лесохозяйств. наук, проф.; ResearcherID: AAW-4454-2021,
ORCID: https://orcid.org/0000-0001-7242-656X
Бугае Парк*[3], *руководитель отд. исследований и разработок;
ORCID: https://orcid.org/0000-0002-4626-2351
Агус Харьянто*[1], *д-р техн. наук, проф.; ORCID: https://orcid.org/0000-0002-8954-4463
[1]Университет Лампунга, г. Бандар-Лампунг, пров. Лампунг, Индонезия;
wahyu.hidayat@fp.unila.ac.id✉, fadillamarthaa@gmail.com, indra.gumay@fp.unila.ac.id, agus.haryanto@fp.unila.ac.id
[2]Национальное агентство исследований и инноваций Индонезии, Южный Лампунг, Индонезия; hend051@brin.go.id
[3]Компания SunBrand Industrial Inc., пров. Чолла-Намдо, Республика Корея;
bu2000@hanmail.net

Поступила в редакцию 09.01.26 / Одобрена после рецензирования 03.04.26 / Принята к печати 06.04.26

Аннотация. Газификация каучуковых (*Hevea brasiliensis*) гранул представляет собой перспективный способ преобразования избыточного количества лигноцеллюлозной биомассы в источник энергии. Помимо производства синтезного газа (сингаза), процесс приводит к образованию побочных продуктов, таких как смола и биоуголь, которые требуют комплексной характеристики для оптимизации процессов и дальнейшего использования. Газификатор с нисходящим потоком был выбран потому, что он производит меньше смолы, чем газификаторы других типов. Целью данного исследования

© Хидаят В., Амелия Ф.М., Прасетиа Х., Фебрияно И.Г., Парк Б., Харьянто А., 2026
Статья опубликована в открытом доступе и распространяется на условиях лицензии CC BY 4.0

является анализ химического состава и характеристик смолы и биоугля как побочных продуктов газификации древесных гранул *Hevea brasiliensis* с применением газификатора с нисходящим потоком. Химические компоненты смолы анализировали с помощью газовой хроматографии с масс-спектрометрией, а характеристики биоугля – с помощью рентгеновской дифракции, инфракрасной спектроскопии с преобразованием Фурье и автоэмиссионной сканирующей электронной микроскопии / энергодисперсионной рентгеновской спектрометрии. Химический состав смолы включает сложные соединения, в т. ч. карбоновые кислоты, алканы, ароматические углеводороды и фенолы. Спектр инфракрасной Фурье-спектроскопии показывает, что биоуголь характеризуется функциональными группами, ассоциированными с насыщенными кислородом углеводами, которые отражают структурные компоненты углеводов, целлюлозы и гемицеллюлозы (C−O, C=O, C−H, C=C, C≡C и C−N). На диаграмме рентгеновской дифракции видно 4 дифракционных пика, включая 2 резких и интенсивных пика (2θ = 28° и 40°) с максимальной кристалличностью пика 71,73 % и размером кристалла 5,47 нм. Структура биоугля проанализирована с помощью сканирующей электронной микроскопии при увеличении 1000× и 5000×, что позволило выявить относительно плоскую, менее пористую поверхность. В биоугле обнаружены такие химические элементы, как углерод, кислород, алюминий, кремний, калий, кальций и железо. Основной элемент – углерод с атомным процентом 80,97 %.

Ключевые слова: деготь, биоуголь, газогенератор с нисходящим потоком, древесные гранулы из каучука, газовая хроматография-масс-спектроскопия, рентгеновская дифракция, инфракрасная Фурье-спектроскопия, автоэмиссионная сканирующая электронная микроскопия / энергодисперсионная рентгеновская спектрометрия

Благодарности: Авторы выражают искреннюю признательность Корейскому институту энергетических исследований (KIER) за предоставление газификатора мощностью 20 кВт и генератора синтез-газа в рамках гранта № KIER-2023-05-03-01, что в большой степени поспособствовало успешному завершению данного исследования.

Для цитирования: Хидаят В., Амелия Ф.М., Прасетиа Х., Фебрияно И.Г., Парк Б., Харьянто А. Характеристика дегтя и биоугля при газификации гранул *Hevea brasiliensis* // Изв. вузов. Лесн. журн. 2026. № 5. С. 152–166.
https://doi.org/10.37482/0536-1036-2026-5-152-166

Introduction

Energy use in Indonesia is very high and has increased by approximately 7 % over the past decade. The increase in primary energy demand is influenced by economic and population growth [17]. Fossil fuels account for approximately 95 % of Indonesia's total energy consumption, with oil contributing around 50 % of the country's total energy production [2]. Excessive consumption of fossil fuels creates environmental problems and, if continued, will deplete available resources, leading to fuel scarcity [3, 12]. In the long term, the availability of fossil fuels is expected to continue declining, necessitating the use of alternative, renewable, and environmentally friendly energy sources. As of 2026, the share of new and renewable energy in Indonesia remains below the 23 % target set for 2025, highlighting the need to accelerate its development in line with the national target of increasing the share to 31 % by 2050, as outlined in the National Energy Plan (RUEN) [32]. Alternative energy, also known as renewable energy, is energy derived from renewable, environmentally friendly sources, such as natural sources and biomass.

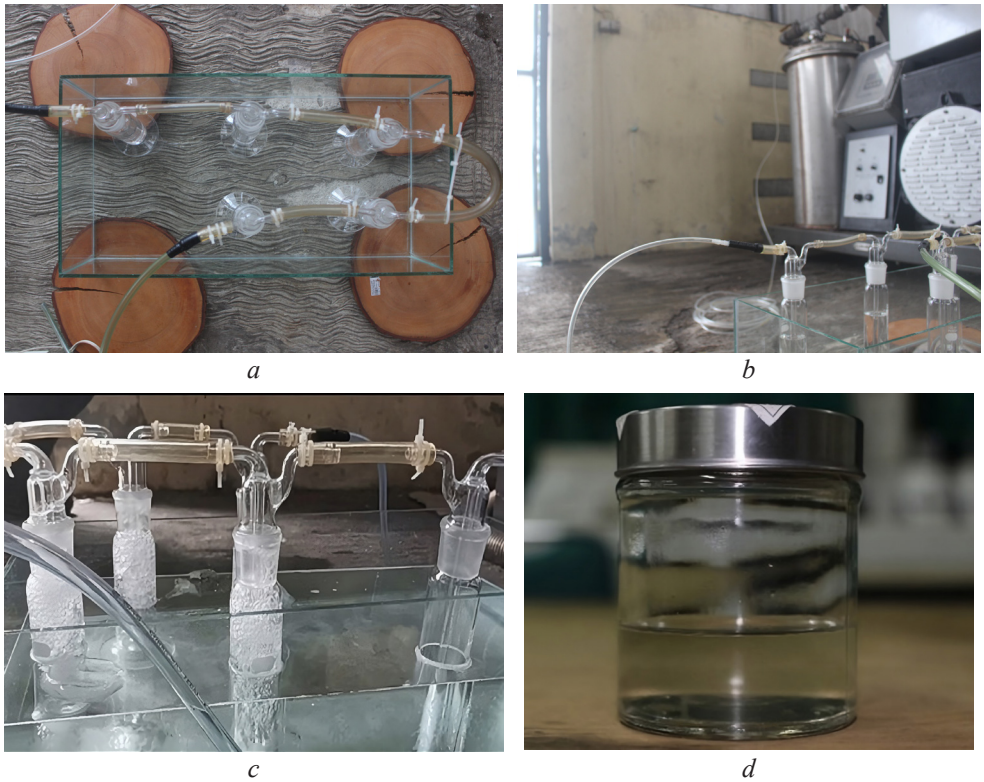
Biomass is organic material produced by photosynthesis as a product or as waste [37]. Biomass is a renewable resource, making it a sustainable source of alternative energy [27]. One type of biomass with potential for development in Indonesia is rubberwood (*Hevea brasiliensis*). The area covered by rubber trees in Indonesia is 3.4 mln ha, the second-largest rubberwood area in the world [25]. The potential for rubberwood biomass waste from harvesting is approximately 5 % per year, or 34 mln m^3/year. Generally, wood biomass is bulky, so it needs to be densified into pellets to make it more practical to use [6]. Pellets, as a source of biomass energy, offer several advantages over other types of biomass, such as firewood and sawmill waste, particularly in terms of their higher density and more uniform shape. This high density results in increased energy-conversion efficiency [15].

Biomass conversion technology is generally divided into three types: direct combustion, biochemical conversion, and thermochemical conversion. Thermochemical technology converts biomass into fuel through thermal treatment processes such as pyrolysis, gasification, liquefaction, and carbonization. Gasification is the most effective thermal technology for converting biomass into gas, compared with pyrolysis and carbonization. Gasification reactors (gasifiers) have several types distinguished by the direction of air flow: downdraft, updraft, crossdraft, bed-fluidized downdraft, and inverted downdraft. The downdraft gasifier was chosen because it offers several advantages, including cleaner gas combustion, easier operation, and the ability to utilize various types of biomass [46]. This study aims to analyze the chemical components and characteristics of tar and biochar as by-products from wood (*Hevea brasiliensis*) pellet gasification using a downdraft gasifier.

Research Objects and Methods

A total of 1,174 kg of rubberwood (*Hevea brasiliensis*) pellets were used in this study, obtained from PT IGJ Wood Pellet in Lampung. The tools used in the study included a 15 kW downdraft gasifier reactor, flame gun, portable gas, spray bottle, biosolar, isopropanol liquid, air pump, 200-mesh sieve machine, zip plastic, impinger tube, 20 × 30 cm condensation glass, silicone hose, Thermogravimetric Analyzer (TGA801, LECO Ltd., Netherlands), Bomb Calorimeter (6400 Automatic Isoperibol Calorimeter, Parr Instrumental Company Ltd., USA), Automatic Elemental Analyzer (Elementar America Inc., New York), GCMS Shmadzu GCMS-QP2010 Ultra, Bruker type Inventio-R, PANalytical X'Pert 3 Powder, and FE-SEM Thermo Scientific Quattro S machine.

Preparation of tools and materials, as well as tar sampling from syngas using an impinger tube system containing isopropanol as the absorbing solution, was carried out at the laboratory workshop of forest product technology, Faculty of Agriculture, University of Lampung (fig. 1). An assembly of five 100 mL impinger tubes, with tubes 1–4 filled with 50 mL of isopropanol solution and the fifth left empty, was placed in a condensation glass filled with cold water (fig. 1*c*). A silicone tube was connected from the gasifier outlet valve to the first impinger tube to allow gas to enter the system (fig. 1*b*). Another tube was attached to the opposite end of the impinger tube assembly and connected to an air pump (fig. 1*b*). The air pump was then operated for 60 minutes, resulting in the continuous bubbles formation in each impinger tube (fig. 1*c*). Afterward, the isopropanol solution from all impinger tubes was transferred into a 50 mL glass bottle and analyzed using GC-MS to determine its chemical composition.



a *b*

c *d*

Fig. 1. Tar sampling scheme: *a* – overall setup; *b* – connection to gasifier outlet; *c* – impinger tube system in cold-water bath; *d* – collected tar sample in isopropanol

Biochar was obtained from the gasifier ash vessel by opening the cover and removing the material. The samples were collected one day after gasifier operation to ensure safe handling, as freshly produced biochar remains hot and may ignite, and were then ground using a blender and sieved through a 200-mesh sieve. The prepared biochar was placed in sealed plastic bags and weighed using a digital scale. The samples were then analyzed at the mineral technology research laboratory of the National Research and Innovation Agency in Lampung using FTIR, XRD, and FE-SEM/EDS analyses.

The parameters used in this study were Gas Chromatography Mass Spectrometer (GCMS) analysis of the chemical components of tar, Fourier Transform Infrared (FTIR) analysis to determine the functional groups of biochar, X-Ray Diffraction (XRD) analysis to determine the degree of crystallinity distance (d), width (La), height (Lc), and number of aromatic layers (N) in the sample, and Field Emission Scanning Electron Microscopy/Energy Dispersive X-Ray Spectroscopy (FE-SEM/EDS) was used to determine the morphology and surface characteristics of biochar and to characterize its pore structure through cross-sectional analysis visually.

Results and Discussion

GC-MS analysis of the syngas tar revealed the presence of multiple compounds, exhibiting significantly different peak intensities between the main and secondary components (fig. 2).

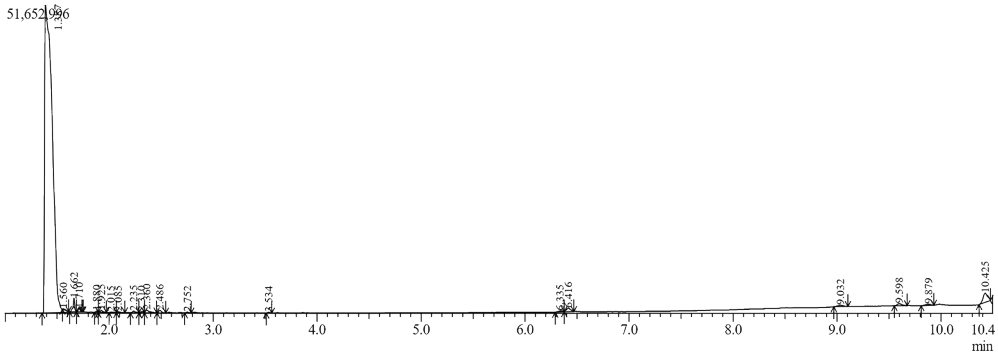


Fig. 2. Chromatogram of tar obtained during the gasification process

The main chemical compounds in tar obtained from gasification include Propanamide, 3,3'-thiobis-, Decane, Toluene, Undecane, Ethylbenzene, p-Xylene, Naphthalene, decahydro-, trans-, Benzene, 1,3-dimethyl-, Benzene, 1-ethyl-3-methyl-, Benzene, 1,2,4-trimethyl-, Bicyclo[4.2.0]octa-1,3,5-triene, Mesitylene, Benzene, 1,2,3-trimethyl-, 1H-Indene, 1-chloro-2,3-dihydro-, n-Hexadecanoic acid, Ethanol, 2-(9-octadecenyloxy)-, (Z), Octadecanoic acid, and Caffeine. These results indicate that tar components comprise a complex mixture of compounds, including carboxylic acids, alkanes, aromatic hydrocarbons, and phenols, with varying percentages, as shown in table 1. Various compounds in tar cause fouling (deposition) and scaling after the gas becomes more saturated. This causes aerosol formation and deposition within the installation, leading to clogging [38]. This clogging can cause engine damage and inhibit the gasification process, resulting in suboptimal products [16]. Knowing the composition of tar can help in selecting appropriate methods for treating and disposing of tar waste.

Based on table 1, tar contains aromatic hydrocarbon compounds, some of which are polycyclic aromatic hydrocarbons (PAHs). The dominant aromatic hydrocarbon compounds in tar waste are decane, toluene, styrene, ethylbenzene, and xylene. The chemical components of tar that are classified as aromatic hydrocarbon compounds are naphthalene, anthracene, fluoranthene, pyrene, indeno, and benzene, which are included in the main PAH compounds. Several previous studies have mentioned that there are five groups of compounds in tar, including GC-undetectable tar, namely heterocyclic, light aromatic (1 ring), light PAH compounds (2–3 rings), and heavy PAH compounds (4–7 rings) [23].

Table 1

Chemical Compounds in Tar

Peak	Area, %	Height, %	Detected Compounds
1	93.45	86.04	*Propanamide, 3,3'-thiobis-*
2	0.09	0.30	*Decane*
3	0.96	3.76	*Toluene*
4	0.24	0.91	*Undecane*
5	0.10	0.37	*Ethylbenzene*
6	0.24	0.58	*p-Xylene*
7	0.06	0.11	*Naphthalene, decahydro-, trans-*
8	0.12	0.25	*Benzene, 1,3-dimethyl-*
9	0.20	0.40	*Benzene, 1-ethyl-3-methyl-*
10	0.16	0.31	*Benzene, 1,2,4-trimethyl-*
11	0.44	0.79	*Bicyclo[4.2.0]octa-1,3,5-triene*

The end of table 1

Peak	Area, %	Height, %	Detected Compounds
12	0.29	0.68	*Mesitylene*
13	0.07	0.21	*Benzene, 1,2,3-trimethyl-*
14	0.06	0.20	*1H-Indene, 1-chloro-2,3-dihydro-*
15	0.23	0.30	*n-Hexadecanoic acid*
16	0.60	0.98	*n-Hexadecanoic acid*
17	0.32	0.39	*Ethanol, 2-(9-octadecenyloxy)-, (Z)*
18	0.38	0.57	*Octadecanoic acid*
19	0.26	0.35	*Caffeine*

Based on table 1, tar contains aromatic hydrocarbon compounds, some of which are polycyclic aromatic hydrocarbons (PAHs). The dominant aromatic hydrocarbon compounds in tar waste are decane, toluene, styrene, ethylbenzene, and xylene. The chemical components of tar that are classified as aromatic hydrocarbon compounds are naphthalene, anthracene, fluoranthene, pyrene, indeno, and benzene, which are included in the main PAH compounds. Several previous studies have mentioned that there are five groups of compounds in tar, including GC-undetectable tar, namely heterocyclic, light aromatic (1 ring), light PAH compounds (2–3 rings), and heavy PAH compounds (4–7 rings) [23].

Primary tar compounds are produced during the pyrolysis stage in gasification by the thermal decomposition of biomass, which produces acids, sugars, alcohols, ketones, aldehydes, phenols, catechols, and oxides [14]. Phenols are the result of the decomposition of cellulose, hemicellulose, and lignin. However, phenols are not classified as carcinogenic compounds, but rather as toxic compounds at certain concentrations [45]. The chemical composition of gasification by-products is influenced by the raw materials and gasification temperature [26].

The decomposition of organic waste yields toxic synthetic organic compounds, resulting in high phenol concentrations [44]. High phenol levels are also caused by the decomposition of organic materials such as wood, livestock feed residues, and organic fertilizers [35]. The phenol content is also influenced by the amount of lignin contained in the raw material because phenol is derived from the decomposition of lignin [13]. The chemical compound content in tar depends on several factors, including the type and composition of biomass, the type of gasifier, and the operating temperature.

Functional groups in biochar must be identified if it is to be considered for further use. The functional groups of compounds in biochar are identified by FTIR analysis, as shown in fig. 3.

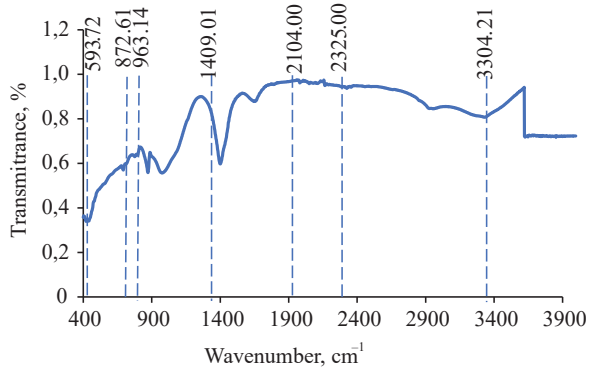


Fig. 3. FTIR spectra of biochar

The peak at 3304.21 cm^{-1} is for the OH group [18]. The presence of hydroxyl (O-H) groups in biochar indicates the formation of strong hydrogen bonds between hydrocarbon compounds and water vapor residues [8]. The next peak is at 2325.00 cm^{-1}, which belongs to C=C alkenes. Alkenes are functional groups that have a high level of carbon purity [42]. The next peak at 2104 cm^{-1} belongs to the ester compound group. Esters are compounds that can be obtained from derivatives between alcohol and carboxylic acid [29]. In high-temperature processes, hemicellulose and cellulose are converted through polymerization. This is indicated by the lignin peak at 1409.01 cm^{-1}, which proves that biochar is composed of lignin and polymers produced at high temperatures [7]. The next peak at 963.14 cm^{-1} belongs to alcohol, while the peak at 900−1000 cm^{-1} indicates C−O compounds [30]. Another peak at 872.61 cm^{-1} is attributed to aromatic C–H stretching [41]. The last peak at 593.72 cm^{-1} reflects the presence of aliphatic compounds mixed with iodine compounds.

The FTIR spectrum exhibits multiple peaks corresponding to various functional groups, as listed in table 2. FTIR spectrum indicates that biochar is characterized by functional groups associated with oxygenated hydrocarbons, reflecting the structural components of carbohydrates, cellulose, and hemicellulose. It was observed that all biochars showed spectral variation, attributed to the gasification process. However, all biochars exhibited similar trends in oxygen-rich functional groups, which are highly desirable for adsorbing pollutants, such as those found in wastewater, dyes, or oils [39]. The presence of polar groups, such as alcohol (OH), ester, ketone, aldehyde, carboxylate, and phenol, indicates that biochar samples could be useful as water pollutant adsorbents and soil ameliorants [31].

Table 2

Functional Groups of FTIR Spectroscopy for Rubberwood Biochar

Wavenumber	Functional Group	Compounds
593.72	C−I	Aliphatic iodine
872.61	CH=CH	Aromatic hydrocarbons
963.14	C−O	Ketones
1409.01	$-NO_2$	Nitro
2104.00	−COO−	Esters
2325.00	C≡C	Alkenes
3304.21	C=H	Aromatic alkenes

XRD analysis was used to analyze the crystallinity of biomass and the structure of biochar. XRD analysis can detect significant changes in the crystal size of carbonized samples over a wide temperature range, from 900 °C to 1500 °C [10]. Fig. 4 shows the diffraction pattern of the biochar formed. Four diffraction peaks are observed, with two quite high and sharp, namely at 2θ values of 28° and 40°, corresponding to cellulose crystal planes in wood [24]. After the first diffraction peak, the subsequent peaks experience a significant decrease in intensity and an increase in width. This decrease indicates that biochar has lost some of its cellulose crystal structure [22].

At 300 °C, biomass decomposes partially, but the crystalline structure of cellulose remains intact because cellulose exhibits good thermal stability. Biochar is destroyed at temperatures above 400 °C, so the diffraction peak is not very pronounced. Higher pyrolysis temperatures produce a broader peak at 2θ of 40°. This diffraction peak arises from a sequential arrangement of aromatic carbons, indicating crystallization and an increase in crystallite size [33]. The formation of aromatic

structures began after the complete decomposition of the wood nanocomposite structure during the combustion process [9].

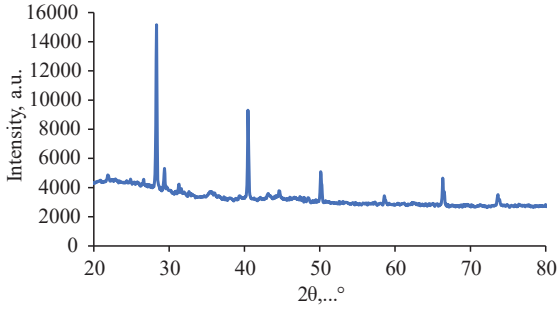


Fig. 4. XRD patterns of biochar from rubberwood pellets

The crystallinity percentage was calculated using the Scherrer equation, which relates the size of nanocrystals in solids to the broadening of diffraction peaks, as shown in table 3, showing that the relative crystallinity of each diffraction peak differs significantly. This difference is due to the calculation of relative crystallinity, which is based on the axial position and determined by the relative amounts of crystalline and amorphous parts in biochar [4]. The relative crystallinity of cellulose increases as the amorphous portion degrades [1]. There is no direct correlation between the cellulose, hemicellulose, and lignin content of biochar and the degree of crystallinity. Lignin and hemicellulose are found in amorphous 2θ between 15° and 22°, while the crystalline portion of cellulose is at 2θ around > 22° [43].

Table 3

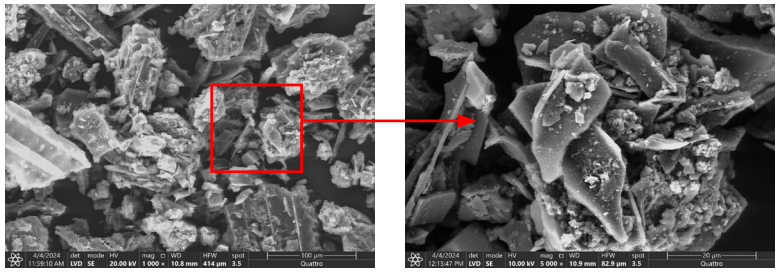
Biochar Relative Crystallinity Percentage and Crystal Width

Peaks	Crystallinity, %	Crystal Width, nm
1	71.73	5.47
2	64.00	5.65
3	33.33	5.85
4	31.25	6.33

This difference is due to the calculation of relative crystallinity, which is based on the axial position and determined by the relative amounts of crystalline and amorphous parts in biochar [4]. The relative crystallinity of cellulose increases as the amorphous portion degrades [1]. There is no direct correlation between the cellulose, hemicellulose, and lignin content of biochar and the degree of crystallinity. Lignin and hemicellulose are found in amorphous 2θ between 15° and 22°, while the crystalline portion of cellulose is at 2θ around > 22° [43].

SEM analysis was used to examine the surface topography of biochar. Fig. 5 shows the surface topography of biochar magnified 1000× and 5000× using SEM. The structure of biochar at 1000× magnification shows randomly scattered pore-like holes with unclear grooves. At 5000× magnification, the surface structure of biochar becomes clearer, revealing flakes and pebble-like shapes. This structure is formed because the micro-pores are filled with tar (condensed volatile substances) and other decomposition products [19]. This is influenced by several factors affecting the biochar produced, including residence time, temperature, and reactor type [5]. Biochar can be used as an adsorbent for heavy metals in soil, as the active sites can attract and bind these toxic elements [40]. The application of biochar can increase

soil porosity by 2–40 % and reduce soil density by 3–30 % [20, 36]. Biochar can also be used in microbial fuel cell technology due to its biocompatibility, high electrical conductivity, and low cost [21].



a *b*

Fig. 5. Surface structure of rubberwood pellet biochar with SEM magnification: *a* –1000×; *b* – 5000×

EDS mapping is generated from characteristic X-rays fired at the position whose composition is to be determined. Peaks corresponding to a particular element will then appear, and the amount of the compound present can be calculated. The results of EDS-SEM scanning at 2500× show the elemental composition of the biochar (fig. 6). Detected elements include carbon, oxygen, aluminium, silicon, potassium, calcium, and iron. The highest detected compound component was carbon, followed by oxygen and other compound elements, as shown in table 4.

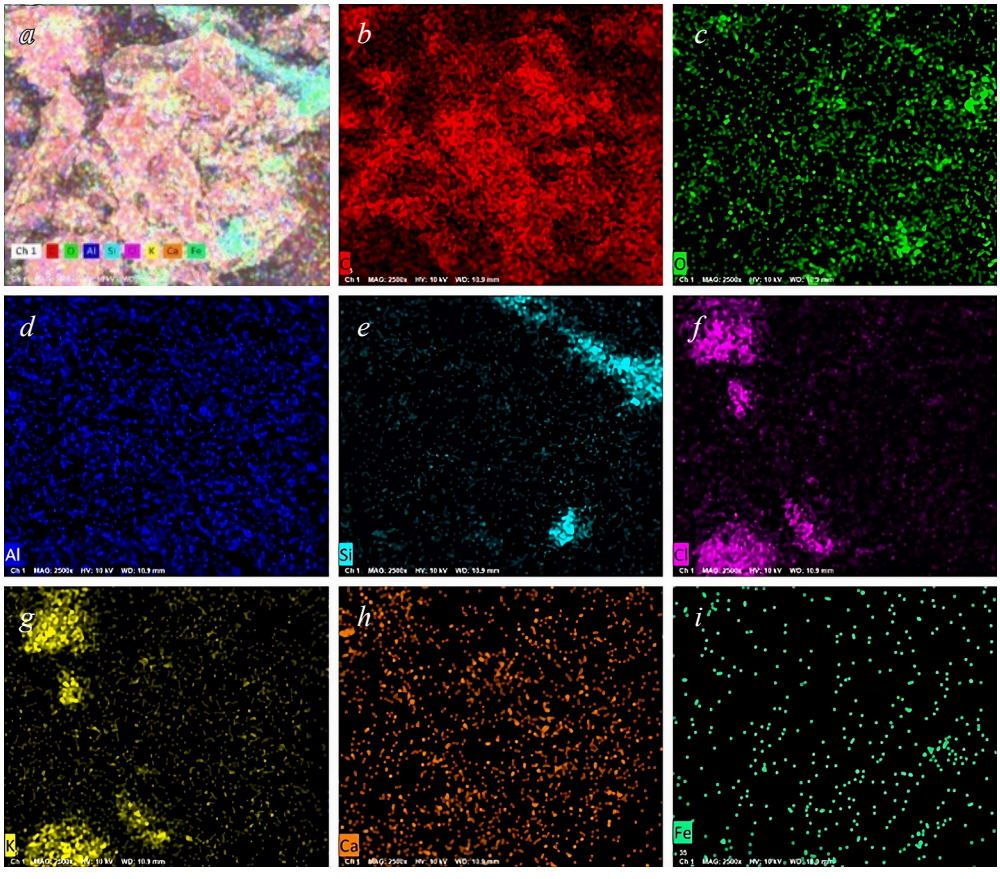


Fig. 6. EDS mapping of biochar compounds: *a* – SEM image (2500×); *b* – carbon; *c* – oxygen; *d* – aluminium; *e* – silicon; *f* – chlorine; *g* – potassium; *h* – calcium; *i* – iron

Table 4

Atomic Value of Biochar Compound Elements

Compounds	Mass, %	Atoms, %
Carbon	48.74	80.97
Oxygen	7.72	9.63
Potassium	5.60	2.86
Chlorine	4.06	2.28
Silicon	2.38	1.69
Calcium	1.86	0.93
Iron	1.79	0.64
Aluminium	1.35	1.00
Total	73.50	100.00

Carbon is the dominant element in biochar, accounting for 80.97 % by atomic percentage, followed by oxygen at 9.63 %. It should be noted that the total mass percentage does not reach 100 % due to EDS limitations, as certain light elements (e.g., hydrogen) are not detected. Biochar consists of 98 % carbon compounds, so carbon and oxygen are commonly found in biochar content because they are the elements that form the graphite structure. Carbon is a highly dynamic element in cation and anion exchange through its four carbon atoms. Each of these carbon atoms then bonds with other atoms to form chain- and ring-shaped compounds [34]. The next elements with relatively high values are potassium (5.60 %), chlorine (4.06 %), and silicon (2.38 %). The remaining elements account for only about 1 % of the total mass. Their composition is shown in fig. 7. It should be noted that the total mass percentage does not reach 100 % due to limitations of EDS analysis, which cannot detect certain light elements (e.g., hydrogen) and may not account for all components in the sample.

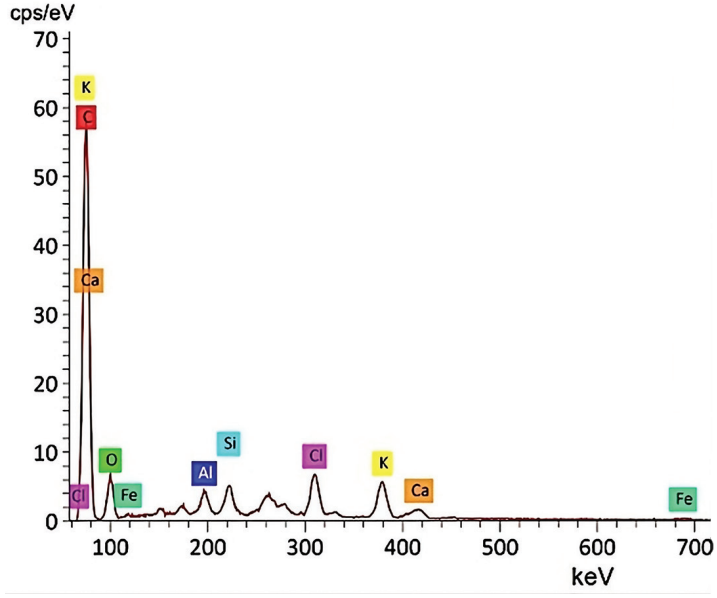


Fig. 7. The energy dispersive X-ray (EDX) spectrum of biochar

Potassium was detected at the highest level, followed by carbon and calcium. Potassium and calcium were detected again at lower peak intensities. Other elements,

such as oxygen, silicon, chlorine, iron, and aluminium, also exhibited low peak intensities. These findings are consistent with most studies, which report that rubberwood pellet biochar contains Mg, P, K, Ca, and O, with some studies also finding small amounts of Si, Fe, and Cl. The presence of K, Ca, and P from biochar helps plants retain soil nutrients and increases soil organic matter [11, 28].

Conclusions

The chemical components of tar are complex compounds, including carboxylic acids, alkanes, aromatic hydrocarbons, and phenols, which can form aerosols and deposits in installations, leading to fouling and slagging as the gas becomes saturated. This clogging can cause engine damage and inhibit the gasification process, resulting in suboptimal products. Biochar produced from the gasification of rubberwood pellets has a relatively flat surface structure and limited porosity, with carbon as the dominant chemical element at 80.97 %. The FTIR spectrum reveals that biochar exhibits C−I, CH=CH, C−O, −NO2, −COO−, C≡C, and C=H functional groups, characteristic of oxygenated hydrocarbons, reflecting the structures of carbohydrates, cellulose, and hemicellulose. XRD analysis reveals four diffraction peaks in the biochar, with two particularly high and sharp peaks at 2θ values of 28° and 40°. These crystallinity peaks have the highest crystallinity (71.73 %) and a crystal width of 5.47 nm. Biochar derived from rubberwood pellets contained high levels of P, C, Ca, Mg, and O, which may improve nutrient retention in soil and increase soil organic matter, making it suitable as a soil ameliorant.

REFERENCES

1. Ahmad M., Lee S.S., Dou X., Mohan D., Sung J.K., Yang J.E., et al. Effects of Pyrolysis Temperature on Soybean Stover- and Peanut Shell-Derived Biochar Properties and TCE Adsorption in Water. *Bioresource Technology*, 2012, vol. 118, pp. 536–544. https://doi.org/10.1016/j.biortech.2012.05.042

2. Aldi N., Casari N., Pinelli M., Suman A., Vulpio A. Performance Degradation of a Shell-and-Tube Heat Exchanger Due to Tar Deposition. *Energies*, 2022, vol. 15, iss. 4, art. 1490. https://doi.org/10.3390/en15041490

3. Altarawneh M., Ali L. Formation of Polycyclic Aromatic Hydrocarbons (PAHs) in Thermal Systems: A Comprehensive Mechanistic Review. *Energy & Fuels*, 2024, vol. 38(22), pp. 21735–21792. https://doi.org/10.1021/acs.energyfuels.4c03513

4. Bourke J., Manley-Harris M., Fushimi C., Dowaki K., Nunoura T., Antal M.J. Do All Carbonized Charcoals Have the Same Chemical Structure? 2. A Model of the Chemical Structure of Carbonized Charcoal. *Industrial & Engineering Chemistry Research*, 2007, vol. 46(18), pp. 5954–5967. https://doi.org/10.1021/ie070415u

5. Chakraborty I., Sathe S.M., Dubey B.K., Ghangrekar M.M. Waste-Derived Biochar: Applications and Future Perspective in Microbial Fuel Cells. *Bioresource Technology*, 2020, vol. 312, art. 123587. https://doi.org/10.1016/j.biortech.2020.123587

6. Chang S., Zhang Z., Cao L., Ma L., You S., Li W. Co-Gasification of Digestate and Lignite in a Downdraft Fixed Bed Gasifier: Effect of Temperature. *Energy Conversion and Management*, 2020, vol. 213, art. 112798. https://doi.org/10.1016/j.enconman.2020.112798

7. Chen C., Liang W., Fan F., Wang C. The Effect of Temperature on the Properties of Hydrochars Obtained by Hydrothermal Carbonization of Waste *Camellia oleifera* Shells. *ACS Omega*, 2021, vol. 6(25), pp. 16546–16552. https://doi.org/10.1021/acsomega.1c01787

8. Chen Y., Zhang X., Chen W., Yang H., Chen H. The Structure Evolution of Biochar from Biomass Pyrolysis and Its Correlation with Gas Pollutant Adsorption Performance. *Bioresource Technology*, 2017, vol. 246, art. 101–109. https://doi.org/10.1016/j.biortech.2017.08.138

9. Fatriasari W., Ridho M.R., Karimah A., Sudarmanto I., Amin Y., Ismayati M., et al. Characterization of Indonesian Banana Species as an Alternative Cellulose Fibers. *Journal of Natural Fibers*, 2022, vol. 19, iss. 16, pp. 14396–14413. https://doi.org/10.1080/15440478.2022.2064394

10. Funke A., Ziegler F. Hydrothermal Carbonization of Biomass: A Summary and Discussion of Chemical Mechanisms for Process Engineering. *Biofuels, Bioproducts and Biorefining*, 2010, vol. 4, iss. 2, pp. 160–177. https://doi.org/10.1002/bbb.198

11. Gholami P., Khataee A., Soltani R.D.C., Bhatnagar A. A Review on Carbon-Based Materials for Heterogeneous Sonocatalysis: Fundamentals, Properties and Applications. *Ultrasonics Sonochemistry*, 2019, vol. 58, art. 104681. https://doi.org/10.1016/j.ultsonch.2019.104681

12. Han J., Kim H. The Reduction and Control Technology of Tar During Biomass Gasification/Pyrolysis: An Overview. *Renewable and Sustainable Energy Reviews*, 2008, vol. 12, iss. 2, pp. 397–416. https://doi.org/10.1016/j.rser.2006.07.015

13. Hossain M.A., Islam M.S., Hassan M.S., Motalib M.A., et al. Feasibility of Solar Pump for Sustainable Irrigation in Bangladesh. *International Journal of Energy and Environmental Engineering*, 2015, vol. 6, no. 2. https://doi.org/10.1007/s40095-015-0162-4

14. Iwuozor K.O., Luque R., Emenike E.C., Adeniyi A.G. Self-Sustaining Valorization of Waste Tree Bark for Simultaneous Biochar, Soot, and Ash Production. *Biofuels, Bioproducts and Biorefining*, 2025, vol. 19, iss. 3, pp. 882–893. https://doi.org/10.1002/bbb.2747

15. Izzatie N.I., Basha M.H., Uemura Y., Hashim M.S.M., Afendi M., Mazlan M.A.F. Co-Pyrolysis of Rubberwood Sawdust (RWS) and Polypropylene (PP) in a Fixed Bed Pyrolyzer. *Journal of Mechanical Engineering and Sciences*, 2019, vol. 13, no. 1, pp. 4636–4647. https://doi.org/10.15282/jmes.13.1.2019.20.0390

16. Jadhav S., Avila J., Schöll M., Kovacs G.G., Kövari E., Skrabana R., et al. A Walk through Tau Therapeutic Strategies. *Acta Neuropathologica Communications*, 2019, vol. 7, art. 22. https://doi.org/10.1186/s40478-019-0664-z

17. Jayanarasimhan A., Pathak R.M., Shivapuji A.M., Rao L. Tar Formation in Gasification Systems: A Holistic Review of Remediation Approaches and Removal Methods. *ACS Omega*, 2024, vol. 9(2), pp. 2060–2079. https://doi.org/10.1021/acsomega.3c04425

18. Jindo K., Mizumoto H., Sawada Y., Sanchez-Monedero M.A., Sonoki T. Physical and Chemical Characterization of Biochars Derived from Different Agricultural Residues. *Biogeosciences*, 2014, vol. 11, iss. 23, pp. 6613–6621. https://doi.org/10.5194/bg-11-6613-2014

19. Karimi A., Naghizadeh A., Biglari H., Peirovi R., Ghasemi A., Zarei A. Assessment of Human Health Risks and Pollution Index for Heavy Metals in Farmlands Irrigated by Effluents of Stabilization Ponds. *Environmental Science and Pollution Research*, 2020, vol. 27, pp. 10317–10327. https://doi.org/10.1007/s11356-020-07642-6

20. Khaledi S., Delbari M., Galavi H., Bagheri H., Chari M.M. Effects of Biochar Particle Size, Biochar Application Rate, and Moisture Content on Thermal Properties of an Unsaturated Sandy Loam Soil. *Soil and Tillage Research*, 2023, vol. 226, art. 105579. https://doi.org/10.1016/j.still.2022.105579

21. Khataee A., Gholami P., Kalderis D., Pachatouridou E., Konsolakis M. Preparation of Novel CeO_2-Biochar Nanocomposite for Sonocatalytic Degradation of a Textile Dye. *Ultrasonics Sonochemistry*, 2018, vol. 41, pp. 503–513. https://doi.org/10.1016/j.ultsonch.2017.10.013

22. Li D., Li C., Fan M., Shao Y., Sun Y., Zhang L., et al. Investigation of Property of Biochar in Staged Pyrolysis of Cellulose. *Journal of Analytical and Applied Pyrolysis*, 2023, vol. 172, art. 105999. https://doi.org/10.1016/j.jaap.2023.105999

23. Liang Y., Zhao X., Ma P.X., Guo B., Du Y., Han X. pH-Responsive Injectable Hydrogels with Mucosal Adhesiveness Based on Chitosan-Grafted-Dihydrocaffeic Acid and Oxidized Pullulan for Localized Drug Delivery. *Journal of Colloid and Interface Science*, 2019, vol. 536, pp. 224–234. https://doi.org/10.1016/j.jcis.2018.10.056

24. Libra J.A., Ro K.S., Kammann C., Funke A., Berge N.D., Neubauer Y., et al. Hydrothermal Carbonization of Biomass Residuals: A Comparative Review of the Chemistry, Processes and Applications of Wet and Dry Pyrolysis. *Biofuels*, 2011, vol. 2, iss. 1, pp. 71–106. https://doi.org/10.4155/bfs.10.81

25. Lyutyy P., Bekhta P., Ortynska G., Sedliačik J. Formaldehyde, Phenol and Ammonia Emissions from Wood/Recycled Polyethylene Composites. *Acta Facultatis Xylologiae Zvolen*, 2017, vol. 59(1), pp. 107–112. https://doi.org/10.17423/afx.2017.59.1.10

26. Matsumoto K., Yanagi T., Oe Y. Recent Advances in the Synthesis of Carboxylic Acid Esters. *Carboxylic Acid – Key Role in Life Sciences*. Ed. by G.I. Badea, G.L. Radu. IntechOpen, 2018, pp. 7–34. http://dx.doi.org/10.5772/intechopen.74543

27. Milne T.A., Evan R.J., Abatzoglu N. *Biomass Gasifier "Tars": Their Nature, Formation, and Conversion*. National Renewable Energy Laboratory Report. Golden, Colorado, NREL, 1998. 68 p. https://doi.org/10.2172/3726

28. Muvhiiwa R., Kuvarega A., Llana E.M., Muleja A. Study of Biochar from Pyrolysis and Gasification of Wood Pellets in a Nitrogen Plasma Reactor for Design of Biomass Processes. *Journal of Environmental Chemical Engineering*, 2019, vol. 7, iss. 5, art. 103391. https://doi.org/10.1016/j.jece.2019.103391

29. Novais S.V., Zenero M.D.O., Barreto M.S.C., Montes C.R., Cerri C.E.P. Phosphorus Removal from Eutrophic Water Using Modified Biochar. *Science of the Total Environment*, 2018, vol. 633, pp. 825–835. https://doi.org/10.1016/j.scitotenv.2018.03.246

30. Onwudili J.A., Nahil M.A., Wu C., Williams P.T. High Temperature Pyrolysis of Solid Products Obtained from Rapid Hydrothermal Pre-Processing of Pinewood Sawdust. *RSC Advances*, 2014, vol. 4, iss. 66, pp. 34784–34792. https://doi.org/10.1039/C4RA04761C

31. Pereira V.V., Morales M.M., Pereira D.H., de Rezende F.A., de Souza Magalhães C.A., de Lima L.B., et al. Activated Biochar-Based Organomineral Fertilizer Delays Nitrogen Release and Reduces N_2O Emission. *Sustainability*, 2022, vol. 14, iss. 19, art. 12388. https://doi.org/10.3390/su141912388

32. *Presidential Regulation No. 22/2017 on the National Energy Plan (RUEN)*. Government of Indonesia. 2017. 6 p. Available at: https://jdih.esdm.go.id/common/dokumen-external/Perpres%2022%20Tahun%202017.pdf (accessed 05.10.26). (In Indonesian).

33. Reza M.S., Afroze S., Bakar M.S., Saidur R., Aslfattahi N., Taweekun J., Azad A.K. Biochar Characterization of Invasive *Pennisetum purpureum* Grass: Effect of Pyrolysis Temperature. *Biochar*, 2020, vol. 2, pp. 239–251. https://doi.org/10.1007/s42773-020-00048-0

34. Shi L., Sessim M., Tonks M.R., Phillpot S.R. High-Temperature Oxidation of Carbon Fiber and Char by Molecular Dynamics Simulation. *Carbon*, 2021, vol. 185, pp. 449–463. https://doi.org/10.1016/j.carbon.2021.09.038

35. Smith B.C. The Infrared Spectra of Polymers, VI: Polymers with C-O Bonds. *Spectroscopy*, 2022, vol. 37, iss. 5, pp. 15–19. https://doi.org/10.56530/spectroscopy.ly3071f5

36. Usowicz B., Lipiec J., Łukowski M., Marczewski W., Usowicz J. The Effect of Biochar Application on Thermal Properties and Albedo of Loess Soil under Grassland and Fallow. *Soil and Tillage Research*, 2016, vol. 164, pp. 45–51. https://doi.org/10.1016/j.still.2016.03.009

37. Valderrama Rios M.L., González A.M., Lora E.E.S., Almazán del Olmo O.A. Reduction of Tar Generated during Biomass Gasification: A Review. *Biomass and Bioenergy*, 2018, vol. 108, pp. 345–370. https://doi.org/10.1016/j.biombioe.2017.12.002

38. Vinturelle R., Cabral T.S., Oliveira P.C.O.d., Salles J., Faria J.V., Teixeira G.P., et al. Slow Pyrolysis of *Terminalia catappa* L. Municipal Solid Waste and the Use of the Aqueous

Fraction Produced for Bovine Mastitis Control. *Biochemistry and Biophysics Reports*, 2024, vol. 38, art. 101704. https://doi.org/10.1016/j.bbrep.2024.101704

39. Wang K., Remón J., Jiang Z., Ding W. Recent Advances in the Preparation and Application of Biochar Derived from Lignocellulosic Biomass: A Mini Review. *Polymers*, 2024, vol. 16, iss. 6, art. 851. https://doi.org/10.3390/polym16060851

40. Wijitkosum S., Jiwnok P. Elemental Composition of Biochar Obtained from Agricultural Waste for Soil Amendment and Carbon Sequestration. *Applied Sciences*, 2019, vol. 9, iss. 19, art. 3980. https://doi.org/10.3390/app9193980

41. Xiao L.-P., Shi Z.-J., Xu F., Sun R.-C. Hydrothermal Carbonization of Lignocellulosic Biomass. *Bioresource Technology*, 2012, vol. 118, pp. 619–623. https://doi.org/10.1016/j.biortech.2012.05.060

42. Xue Y., Guo Y., Zhang X., Kamali M., Aminabhavi T.M., Appels L., et al. Efficient Adsorptive Removal of Ciprofloxacin and Carbamazepine Using Modified Pinewood Biochar – A Kinetic, Mechanistic Study. *Chemical Engineering Journal*, 2022, vol. 450, part 1, art. 137896. https://doi.org/10.1016/j.cej.2022.137896

43. Yin Q., Liu M., Ren H. Biochar Produced from the Co-Pyrolysis of Sewage Sludge and Walnut Shell for Ammonium and Phosphate Adsorption from Water. *Journal of Environmental Management*, 2019, vol. 249, art. 109410. https://doi.org/10.1016/j.jenvman.2019.109410

44. Zhang J., Huo H., Zhang L., Yang Y., Li H., Ren Y., et al. Effect of High-Temperature Hydrothermal Treatment on the Cellulose Derived from the *Buxus* Plant. *Polymers*, 2022, vol. 14, iss. 10, pp. 2053. https://doi.org/10.3390/polym14102053

45. Zhao Z., Yan H., Gu L. An Electrocatalytic Mono-Functionalization of Alkenes towards Alkenyl Selenium Sulfonates. *Chemical Communications*, 2025, vol. 61, iss. 19, pp. 3868–3871. https://doi.org/10.1039/d4cc06246a

46. Ziolkowska A., Debska B., Banach-Szott M. Transformations of Phenolic Compounds in Meadow Soils. *Scientific Reports*, 2020, vol. 10, art. 19330. https://doi.org/10.1038/s41598-020-76316-7

Конфликт интересов: Авторы заявляют об отсутствии конфликта интересов
Conflict of interest: The authors declare no conflict of interest

Вклад авторов: Все авторы в равной доле участвовали в написании статьи
Authors' Contribution: All authors contributed equally to the manuscript